Stochastic and coherence resonance in feed-forward-loop neuronal network motifs

Daqing Guo*
Centre for Nonlinear and Complex Systems, School of Electronic Engineering, University of Electronic Science and Technology of China, Chengdu 610054, People's Republic of China

Chunguang Li†
Department of Information Science and Electronic Engineering, Zhejiang University, Hangzhou 310027, People's Republic of China
(Received 26 March 2009; published 27 May 2009)

The relationships between noise and complex dynamic behaviors of neuronal ensembles are key questions in computational neuroscience, particularly in understanding some basic signal transmission mechanisms of the brain. Here we systemically investigate both the stochastic resonance (SR) and coherence resonance (CR) in the triple-neuron feed-forward-loop (FFL) network motifs by computational modeling. We use the Izhikevich neuron model as well as the chemical coupling to build the FFL motifs, and consider all possible motif types. The simulation results demonstrate that these motifs can exploit noise to enrich its dynamic performance. With a proper choice of noise intensities, both the SR and CR can be exhibited in many types of the FFLs. On the other hand, our results also indicate that the coupling strength serves as a control parameter, which has great impacts on the stochastic dynamics of the FFL motifs. Additionally, biological implications of presented results in the field of neuroscience are outlined.

DOI: 10.1103/PhysRevE.79.051921 PACS number(s): 87.19.L−, 05.45.−a, 87.10.−e

I. INTRODUCTION

Complex networks are ubiquitous in both natural and engineered systems. Intensive statistical studies have revealed that a large number of complex networks contain some significantly recurring nontrivial patterns of interconnections [1–3], termed "network motifs," which are believed to be basic building blocks of these networks. Network motifs are currently being widely studied across many scientific disciplines and suggested to perform specific functional roles. In recent years, systematic research works on neuroscience have demonstrated that these motifs do exist in real biological networks, such as neuronal networks [1,3,4], transcription regulatory networks [2,5], protein-protein interaction networks [6], and brain functional networks [7]. Moreover, it is found that, in many systems studied so far, the motifs are linked to each other in a way that does not spoil the independent function of each motif [8]. Elucidating the dynamics and special functions of these network motifs can be therefore treated as the first step to understand the behaviors of whole networks.

On the other hand, neurons are fundamental elements constituting biological neural networks. The main function of neurons is to generate electrical signals in response to chemical and other inputs, and transmit them to other neurons [9]. The constructive effects of noise on signal transmission among neurons have been extensively studied from both theoretical and computational approaches, and many noise-induced complex dynamic behaviors have been found—for example, the synchronization [10–13], stochastic resonance (SR) [14–17], and coherence resonance (CR) [11,18–22]. Among these behaviors, SR and CR are two counterintuitive but rather important phenomena. In the phenomenon of SR, a small periodic signal forcing nonlinear system can be amplified by the addition of a stochastic force, or external noise, to the signal [21,23]. In essence, SR is based on the cooperative effect between the stochastic dynamical system and the external forcing [24,25]. CR reflects the coherent motion stimulated by the intrinsic dynamics of the system [18,26]. Without a periodic signal, coherent oscillation in a nonlinear system can be purely induced by the noise, and the regular behavior of the stochastic dynamics achieve maximum at an appropriate noise level. Both the SR and CR occur in a number of experimental systems [27,28], and are considered to be two basic mechanisms that neurons use to transmit signals.

The triple-neuron feed-forward-loop (FFL) is one of the most significant neuronal network motifs [3], in which, as shown in Fig. 1(a), neuron 1 drives neuron 2, and neurons 1 and 2 both drive neuron 3. In this motif, neuron 1 and 3 can be considered as the input and output neurons, respectively. In general, neurons can be divided into excitatory and inhibitory neurons. Excitatory neurons encourage the activity of neurons on which they act, while inhibitory neurons act in an opposite manner. Depending on whether the neurons in the FFL are excitatory or inhibitory, there are eight possible structural configurations, which are given in Table I. Recently, in [29], simulation results on neuronal network motifs

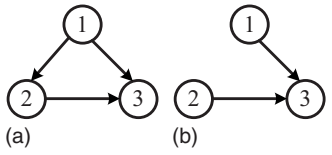

FIG. 1. Connection patterns: (a) the FFL neuronal network motif: neuron 1 drives neuron 2, and both jointly drive neuron 3; (b) simple drive of neuron 3 by neurons 1 and 2 as a comparison of the FFL.

*dqguo@uestc.edu.cn
†Corresponding author; cgli@zju.edu.cn

TABLE I. Eight possible FFL types. Here E and I are used to represent excitatory and inhibitory neurons, respectively.

Type	Neuron 1	Neuron 2	Neuron 3
T1-FFL	E	E	E
T2-FFL	E	I	E
T3-FFL	E	E	I
T4-FFL	E	I	I
T5-FFL	I	E	E
T6-FFL	I	I	E
T7-FFL	I	E	I
T8-FFL	I	I	I

have found some interesting functional roles for them. For instance, the T2-FFL can both accelerate the response to the ON step and delay the response to the OFF step of the input to neuron 1; the mixed-feed-forward-feedback-loop (MFFL) motifs can serve as both the long-term and short-term memories. These results indicate that neuronal network motifs may perform some specific signal processing functions. However, the work in [29] did not consider the effects of noise. Since the nontrivial effects of noise on nonlinear systems, it is reasonable to believe that noise influences the stochastic dynamics of these neuronal network motifs, including the FFLs.

Following this motivation, in this paper, we use computational modeling to systemically study both the SR and CR in the FFL neuronal network motifs. Only neurons coupled via chemical synapses are examined because the case of electrical coupling arising via gap junction is generally bidirectional. In order to fully understand the effects of different types of chemical synapses, all possible FFL types are examined in this work. The rest of this paper is organized as follows. Section II is devoted to introduce the Izhikevich neuron model and the chemical coupling as its main ingredient. Brief simulation results on both the SR and CR in the FFL neuronal network motifs are reported in Sec. III. Finally, a brief conclusion and discussion of our work are given in Sec. IV.

II. MODEL

Let us consider building the FFL neuronal network motifs and performing simulations by using the Izhikevich neuron model [30]. The dynamics of this model is described by the following two equations:

$$\frac{dv_i}{dt} = 0.04v_i^2 + 5v_i + 140 - u_i + I_i, \tag{1}$$

$$\frac{du_i}{dt} = a(bv_i - u_i), \tag{2}$$

with the auxiliary after-spike resetting

$$\text{if} \quad v_i \geq 30 \ \text{mV}, \quad \text{then} \begin{cases} v_i \leftarrow c, \\ u_i \leftarrow u_i + d, \end{cases} \tag{3}$$

where $i=1, 2, 3$ index the neurons, v_i denotes the membrane potential of the neuron, u_i represents the membrane recovery variable, whereas I_i is the total input current. Four dimensionless parameters a, b, c, and d are used to determine the neuron type. According to Ref. [30], we use the regular spiking (RS) neuron ($a=0.02$, $b=0.2$, $c=-65$, and $d=8$) to model the excitatory neuron and fast spiking (FS) neuron ($a=0.1$, $b=0.2$, $c=-65$, and $d=2$) to model the inhibitory neuron, respectively. Both the RS and FS neurons fire very regularly when they are driven by a low suprathreshold dc current. However, as shown in Fig. 2, they can fire burst if the stimulus is strong enough. Whenever the membrane potential reaches a threshold $V_{th}=30$ mV, an action potential is generated, and then the membrane potential and recovery variable are reset according to Eq. (3).

The total input current consists of three terms, which is given by

$$I_i = I_i^{ext} + I_i^{syn} + I_i^{noise}. \tag{4}$$

Here, I_i^{ext} is the external applied current, and I_i^{syn} is the total synaptic current. The noise current $I_i^{noise}=\sqrt{2D}\xi_i(t)$ represents the external or intrinsic fluctuations of the neuron itself, where the Gaussian white noise $\xi_i(t)$ satisfies zero mean $\langle \xi_i(t) \rangle = 0$ and unit variance $\langle \xi_i(t)\xi_i(t+\tau) \rangle = \delta(\tau)$, and D is referred to as the noise intensity.

For the chemical coupling considered in this work, neurons transmit signals with the help of neurotransmitters. In this coupling type, the synaptic current onto neuron i is the linear sum of the currents of all incoming synapses, $I_i^{syn} = \Sigma_j I_{ij}^{syn}$ where the individual synaptic currents are

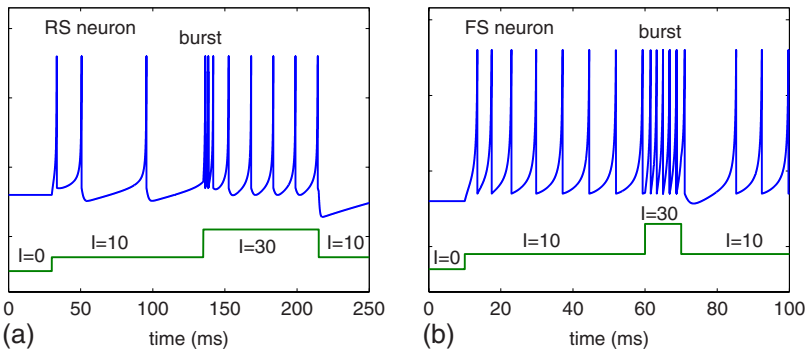

FIG. 2. (Color online) Voltage responses of the Izhikevich neuron to the external current I: (a) regular spiking (RS) neuron and (b) fast spiking (FS) neuron.

$$I_{ij}^{syn}(t) = g_{ij} r_j [E_s - v_i(t)], \tag{5}$$

where v_i represents membrane potential of neuron i, and g_{ij} describes the coupling strength of the synapse from neuron j to neuron i. For simplicity, we assume that $g_{ij}=g$, that is, the coupling strength is identical for all connections. The parameter E_s is the reversal potential which determines the type of synapse. For excitatory synapse, $E_s=0$ mV and for inhibitory synapse, $E_s=-80$ mV. The synapse variable r_j is the fraction of postsynaptically bound neurotransmitter. Here we assume r_j obey the first-order kinetics, which is defined by

$$\frac{dr_j}{dt} = F(v_j)(1 - r_j) - \frac{r_j}{\tau_s}, \tag{6}$$

where $F(v_j)=1/[1+\exp(-v_j)]$ is the synaptic recovery function and $\tau_s=10$ ms is the synaptic decay rate.

III. NUMERICAL RESULTS

The above-mentioned stochastic differential Eqs. (1) and (2) are numerically integrated using the Euler-Maruyama algorithm [31] with a fixed time step $h=0.1$ ms. Since neuron 1 and 3 are repetitively regarded as the input and output neurons of the FFL neuronal network motif, we only examine the response of neuron 3 to the external applied current of neuron 1. To quantitatively evaluate the performances of SR and CR, several effective measures are introduced. The data shown in our work are averaged results of 20 independent runs.

Let us first examine whether the stochastic resonance can be exhibited in the FFL neuronal network motifs. In order to do this, we set $I_2=I_3=2$ and consider that neuron 1 is subject to a local weak periodic forcing, that is $I_1=I_0+C\sin(2\pi f_s t)$, where $I_0=2$ is the bias current, $C=1$ is the amplitude, and f_s is the frequency of the signal. Under the circumstance, the external applied currents are too weak to excite the FFLs in the absence of noise. Here we use the signal-to-noise ratio (SNR) to measure the relative performance of SR quantitatively. To calculate the SNR, the power spectral density (PSD) should be obtained from the time series of the output neuron. An example of the stochastic oscillation in the T1-FFL motif is plotted in Figs. 3(a) and 3(b). As we see, the PSD consists of two main components: (a) a main peak located at the forcing frequency and several other peaks located at multiples of the forcing frequency; and (b) a background noise. This indicates that the frequency characteristic of the output spike train is induced by the local weak periodic forcing. Then the SNR β is simply defined as, $\beta=[S(f_s)-N(f_s)]/N(f_s)$, where f_s is the input signal frequency, $S(f_s)$ is the power at the frequency f_s, and $N(f_s)$ is the averaged power at nearby frequencies. Note that there are several ways to define the SNR, but variations of this definition do not qualitatively affect the final results.

Now we study the dependence of SNR on the noise intensity as well as the coupling strength. Since the SNR is too low when neuron 1 is inhibitory, we only find interesting results for the FLL motifs with excitatory input neuron. The corresponding simulation results are shown in Figs. 4(a) and 4(b). As the noise intensity increases, the SNR curves all first rise and then drop, indicating that such stochastic oscillation shows the best performance at an optimal noise level. The results clearly illustrate the occurrence of stochastic resonance. When the coupling is very weak ($g=0.15$), it obvious that a part of information is lost during the transmission [Fig. 5(a)]. In this case, the abilities of weak periodic signal detection in all considered types are quite low. However, our simulation results show that the T1-FFL is more efficient than other types of FFL. Actually, in this situation, neuron 2 in the T1-FFL can increase reliability of communication to a certain degree. By increasing g from 0.15 to 0.3, the coupling is so strong that almost each spike from the input neuron causes the output neuron emit a spike [Fig. 5(b)], thus resulting the maximal SNR sharply increases for these motifs.

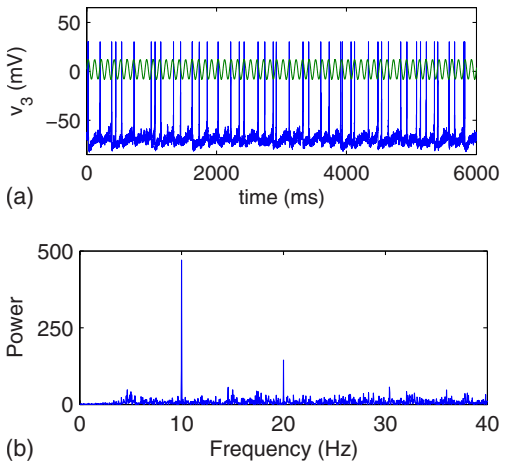

FIG. 3. (Color online) An example of the stochastic oscillation in the T1-FFL, with $D=3$ and $g=0.5$. (a) The time series of v_3 as well as the periodic forcing signal of neuron 1 with frequency $f_s=10$ Hz (for better viewing, the amplitude of the signal is ten times higher than that in the model), and (b) the corresponding power spectrum density graph.

We also study the "simple drive" of neuron 3 by neurons 1 and 2 [Fig. 1(b)] as a reference of comparison. As in the FFL motifs, we use the same method to define the types of the simple drive. In Figs. 4(c) and 4(d), the dependence of SNR on the noise intensity and coupling strength for four corresponding simple drive types are plotted. Similar stochastic resonance can also be seen clearly. There is no big qualitative difference between Figs. 4(b) and 4(d). However, when the coupling is weak [Figs. 4(a) and 4(c)], the maximum of SNR in the T1-FFL (T3-FFL) is obviously larger than those in the T1-Simple (T3-Simple); while the maximum of SNR in the T2-FFL (T4-FFL) is similar with those in the T2-Simple (T4-Simple). The results suggest that for weak coupling the abilities of weak periodic signal detection of the T1-FFL and T3-FFL motifs are more reliable than those of the corresponding simple drive types.

It should be noted that we are especially interested in the results of the T1-FFL and T2-FFL motifs. This is at least due to the following two reasons: (i) since the ratio of excitatory to inhibitory neurons in biological neural networks is about 4:1, the T1-FFL and T2-FFL motifs are more universal than other two types in theory. (ii) The inhibitory output neurons

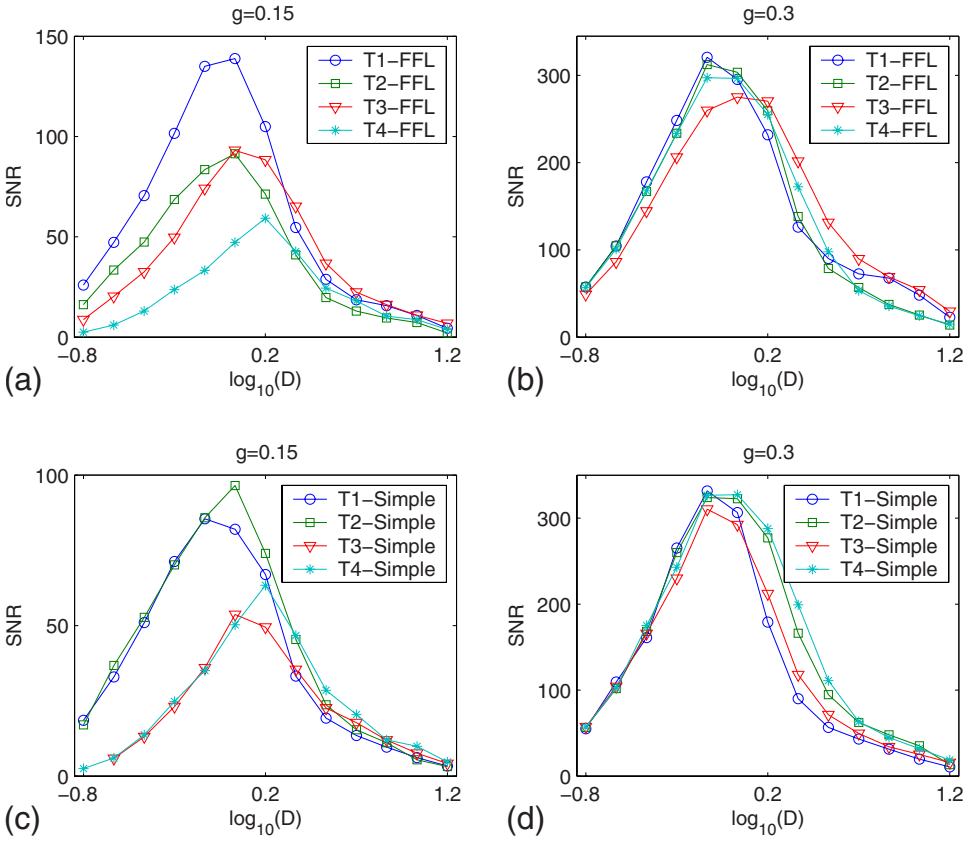

FIG. 4. (Color online) The SNR versus the noise intensity for different FFL and simple drive types, with the periodic signal frequency $f_s=10$ Hz. (a) FFL ($g=0.15$), (b) FFL ($g=0.3$), (c) simple drive ($g=0.15$), and (d) simple drive ($g=0.3$).

in both the T3-FFL and T4-FFL motifs impede any excitatory signals across them, which in principle largely decrease the subsequent propagation of the frequency characteristic.

To further investigate the influence of coupling strength, the maximums of SNR are calculated at the corresponding optimal noise intensities for different values of g. In Fig. 6(a), the maximum of SNR as a function of the coupling strength for both the T1-FFL and T2-FFL motifs are plotted. Figure 6(a) further demonstrates that the T1-FFL is more efficient than the T2-FFL in weak-coupling regime ($g \leq 0.25$). On the other hand, if the coupling strength is larger than 0.4, the T2-FFL shows a better performance. For the T1-FFL, it is clear that the SNR curve exists a local minimum near $g=0.5$. In the case of the T2-FFL, the range of coupling strengths for large values of SNR is much larger, indicating the T2-FFL is more stable and reliable. By comparing the time series in Fig. 5(c) with those in Fig. 5(d), we find that this local minimum is caused by both the irregular burst firing and false firing of the output neuron. At $g=0.5$, a spike from neuron 1 makes both neurons 2 and 3 spiking. For the T1-FFL motif, since neuron 2 is excitatory, the output neuron may fire burst sometimes with the help of noise. But in this case the burst is very sparse and irregular because the coupling is not strong enough. On the other hand, a spike from excitatory neuron 2, which is not caused by the firing of the neuron 1, also leads the output neuron to emit a false spike. The above-mentioned two factors introduce other frequency characteristics in the output spike train. For the T2-FFL motif, the inhibitory neuron 2 can prevent the output neuron firing burst as well as false spike effectively. However, due to synaptic delay, neuron 2 does not prohibit the output neuron emitting the first spike each time. Therefore, the SNR curve of T1-FFL motif exists a local minimum near $g=0.5$. When the coupling strength is increased to a rather large value [for example, $g=0.8$ in Fig. 5(e)], due to strong coupling the burst firing of the output neuron in the T1-FFL motif becomes regular. In this case, the false signals from neuron 2 reduce the SNR, but the regular bursts tend to cancel the decreasing tendency. As a result, the corresponding SNR is enhanced again. The above analysis might explain why there exists a local minimum at the maximum of SNR curve of the T1-FFL motif.

It was recently reported that there exists a special frequency sensitive range for a single neuron [32]. Further works on neuronal networks have demonstrated that these networks display the similar characteristic [33,34]. Here we also investigate the frequency sensitivity of weak periodic signal detection in the FFL neuronal network motifs. Figures 7(a)–7(c) show the output SNR versus the frequency of input signal for different noise levels. In all cases, a bell-shaped SNR curve is seen clearly by tuning the frequency of the input signal, which implies that the ability to detect and transmit signal can be significantly improved when its frequency falls within a special range. On the other hand, the frequency sensitivity of the FFL motifs also relies heavily on noise intensity. As D grows, the top region of the SNR curves all first becomes wide and then becomes narrow. It is obvious that at intermediate noise intensities the SNR for the frequency in a wide range (about 6–20 Hz) has large value. The results suggest that the SR could enhance the effects of weak intrinsic rhythmic oscillations such as the alpha (7.5–13 Hz) and beta (14–25 Hz) rhythms in the brain. The

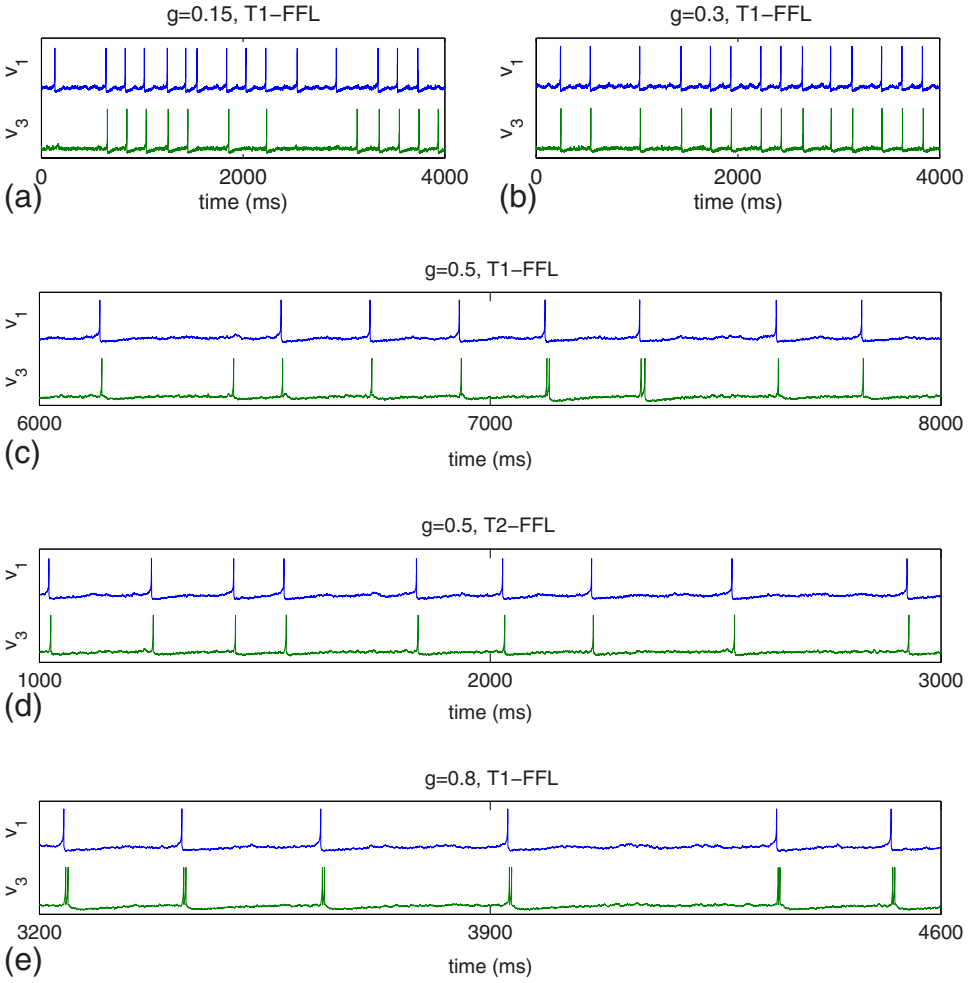

FIG. 5. (Color online) Time series of neurons 1 and 3 for different coupling strengths. (a) T1-FFL ($g=0.15$), (b) T1-FFL ($g=0.3$), (c) T1-FFL ($g=0.5$), (d) T2-FFL ($g=0.5$), and (e) T1-FFL ($g=0.8$). $D=1.08$ and $f_s=10$ Hz in all cases.

above finding may be relevant to the fact that these kinds of oscillations exist widely in the brain of mammals.

Indeed, the frequency sensitive characteristic makes these types of FFL motifs act as a band-pass filter, which implies that they would like to filter out both low-frequency and high-frequency firings but enhance the efficacy of mid-frequency firing. As discussed in Refs. [32–34], this is due to the cooperation of the intrinsic oscillation of the FFL motifs with the periodic input signal.

Next we examine whether the coherence resonance can be exhibited in the FFL neuronal network motifs. In order to do this, we choose $I_1=I_2=I_3=0$ and examine all possible FFL types. We employ a coherence factor, the coefficient of variation, to quantitatively evaluate how the temporal regularity of a spike train is modulated by noise. The coefficient of variation is a dimensionless measure defined as

$$R = \frac{\sqrt{\langle T_k^2 \rangle - \langle T_k \rangle^2}}{\langle T_k \rangle}. \tag{7}$$

Here $\langle \cdot \rangle$ denotes the average over time, $T_k=t_{k+1}-t_k$, and t_k is the time of the kth firing of the neuron. R is related to the timing precision of the information processing and widely used in the field of neuroscience. Note that a smaller R corresponds to a better spiking regularity.

Now we study the dependence of R on the noise intensity as well as the coupling strength. The corresponding simulation results are depicted in Figs. 8(a)–8(h), respectively. As a reference of comparison, the coherence factor as a function of the noise intensity for single excitatory and inhibitory Izhikevich neurons is also plotted in Fig. 8(i). When the coupling strength is small (for instance $g=0.1$), the CR indeed occurs in all FFL types at appropriate noise intensities. Under this circumstance, we speculate that the stochastic dynamics of the output neuron is mainly determined by its neuron type as well the noise intensity. As we can see, it is clear that the FFL motifs with excitatory output neuron can obtain better spiking regularity than those with inhibitory

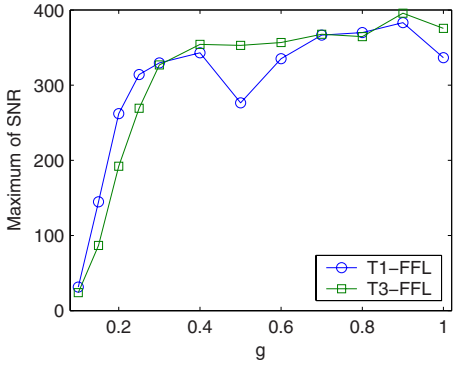

FIG. 6. (Color online) The maximum of SNR as a function of the coupling strength for both the T1-FFL and T2-FFL motifs.

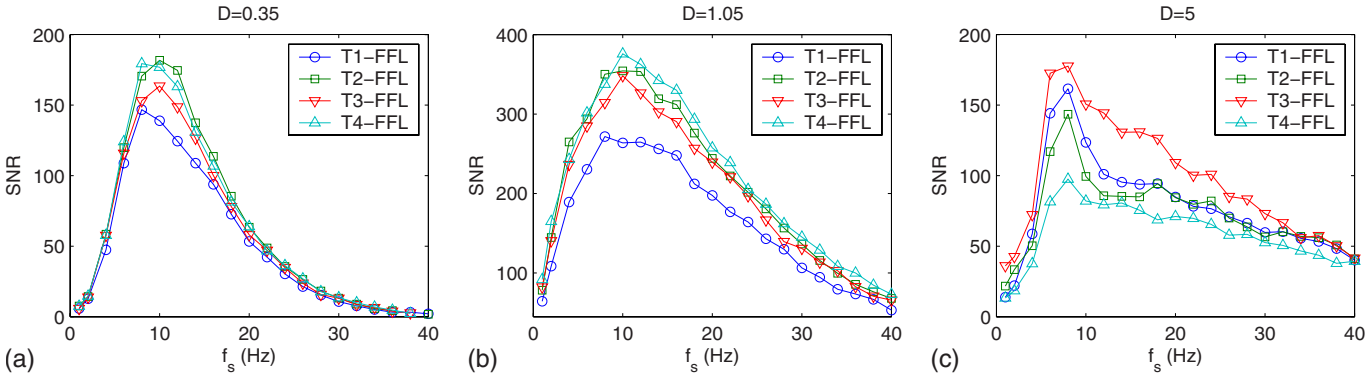

FIG. 7. (Color online) The output SNR versus the frequency of the input signal for different noise intensities. Noise intensities (a) $D=0.35$, (b) $D=1.5$, and (c) $D=5$. $g=0.5$ in all cases.

output neuron, which are quite similar with the results in Fig. 8(i). As the coupling strength grows, the inputs from other neurons start to take command of the stochastic dynamics of the output neuron. If g is increased to a rather large value, such as $g=0.75$, the coupling is so strong that the influences from other neurons cannot be neglected. In this situation, the coherence factors for each considered FFL type become large at corresponding noise intensities, showing depressed temporal coherence. In some worse cases, the CR behaviors even disappear [for example, $g=0.75$ in Figs. 8(c) and 8(g)]. This

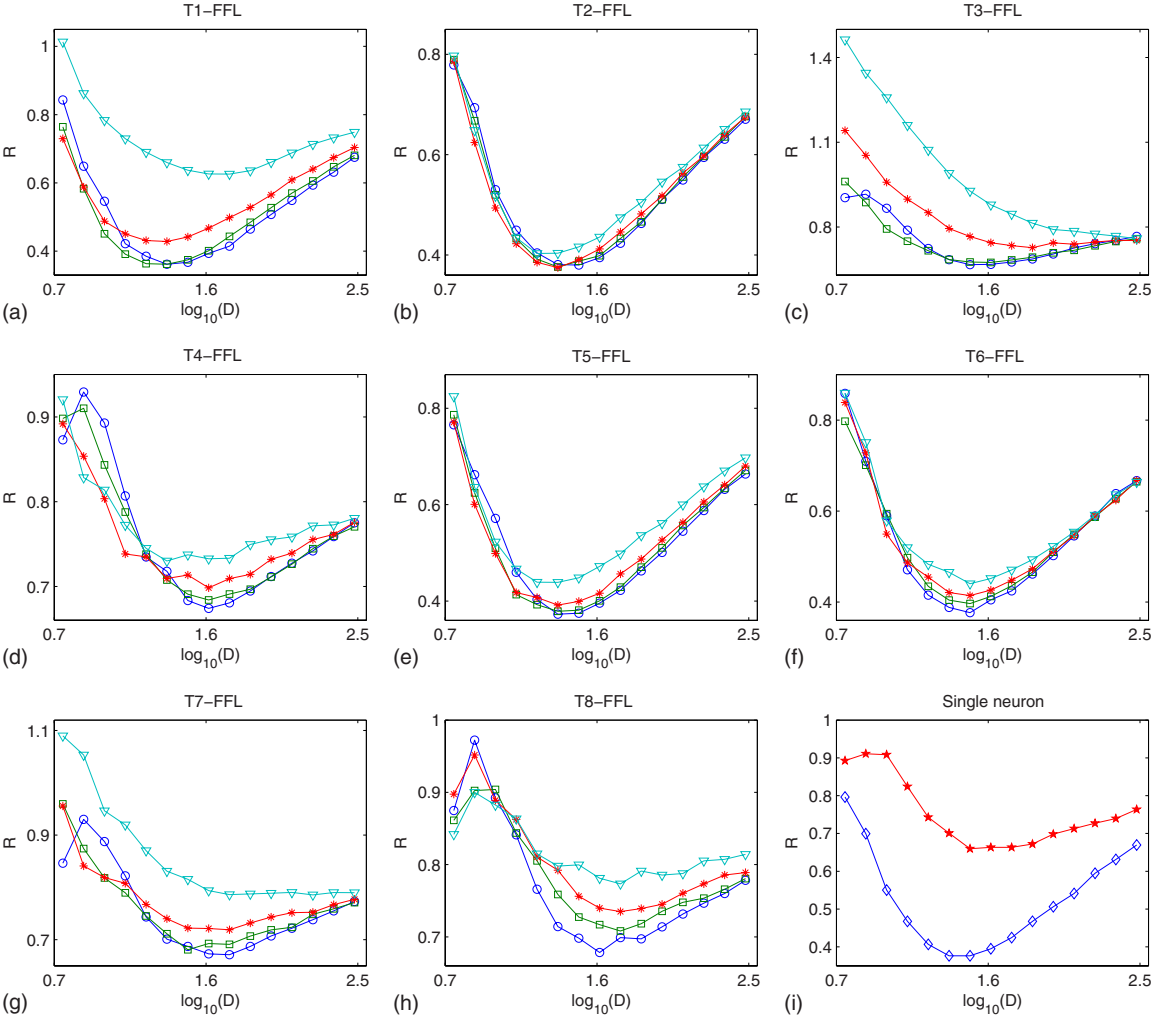

FIG. 8. (Color online) CR in the FFLs and single Izhikevich neuron model. [(a)–(h)] The coherence factor R versus the noise intensity for different coupling strengths. (a) T1-FFL, (b) T2-FFL, (c) T3-FFL, (d) T4-FFL, (e) T5-FFL, (f) T6-FFL, (g) T7-FFL, and (h) T8-FFL. Coupling strengths $g=0.1$ (circle: "○"), $g=0.3$ (square: "□"), $g=0.5$ (asterisk: "*"), and $g=0.75$ (triangle-down: "▽"). (i) The coherence factor R versus the noise intensity for single Izhikevich neuron model. Excitatory neuron (diamond: "◇") and inhibitory neuron (star: "★").

phenomenon is caused by the following two reasons: (i) due to strong coupling, a spike from an excitatory neuron makes the output neuron fire burst, which decreases the average value and increases the variance of the interspike intervals (ISI). (ii) Inhibitory synaptic connections would in principle degrade propagation of the excitations through the neuronal medium. In particular, since the FFLs with neurons $(1,2)=(E,E)$ are much easier to lead the output neuron fire burst in strong-coupling regime, the performances of CR in both the T1-FFL and T3-FFL motifs are much worse than those in other corresponding types.

IV. CONCLUSION AND DISCUSSION

Network motifs provide us a new way to study complex networks. Elucidating these network motifs' dynamics and functions would shed light on the whole networks' behaviors. The present study examined both the stochastic and coherence resonance in the FFL neuronal network motifs via computational modeling. We built the FFL motifs by using the Izhikevich neuron model and the chemical synapse. Depending on whether the neurons in the FFL motifs are excitatory or inhibitory, eight possible structural configurations of the FFLs have been investigated.

In the study of SR, it was observed that only four FFL types can obtain high values of SNR at optimal noise intensities and large coupling strengths. In particular, we found that the T1-FFL is more efficient than the other types of FFLs in weak-coupling regime. However, by comparing the SNR at corresponding coupling strength, it was found that the T2-FFL is more stable and reliable for strong coupling. On the other hand, when the coupling is weak, the abilities of weak periodic signal detection of the T1-FFL and T3-FFL motifs are more reliable than those of the corresponding simple drive types. Moreover, under an intermediate noise, we have shown these types of the FFLs are especially sensitive to input signal with the frequency in the range of about 6–20 Hz. Since the frequency range contains the alpha and beta rhythms, the results might to a certain degree explain why these oscillations exist widely in the brain. In the study of CR, our simulation results demonstrated that CR indeed occurs in all types of the FFLs in weak-coupling regime. However, when the coupling strength is strong, the temporal coherence in all FFL types is seriously deteriorated, which is due to the bursting firing as well as the effect of inhibitory synapse. In some worse cases, the CR behaviors even disappear.

Since the FFL motifs exist widely in real neuronal networks and the noise is ubiquitous in neural systems, the noise-induced complex dynamic behaviors of the FFL motifs presented in this work may have some biological implications. We suggest physiological experiments to test the results and anticipate these results might provide some insights into the neural information transmission mechanism of the FFL neuronal network motifs. Further works on this topic include studying other neuronal network motifs, such as the mixed-feed-forward-feedback loop, as well as considering the electrical coupling case in suitable motifs.

ACKNOWLEDGMENTS

The authors gratefully acknowledge Gang Wang, Bingjie Tao, and Long Sheng for insightful discussions. This work was supported by the National Natural Science Foundation of China (Grant No. NSFC 60871094), the Foundation for the Author of National Excellent Doctoral Dissertation of PR China, and the Youth Foundation of Sichuan Province (Grant No. 07ZQ026-019).

[1] R. Milo, S. Shen-Orr, S. Itzkovitz, N. Kashtan, D. Chklovskii, and U. Alon, Science **298**, 824 (2002).
[2] S. Shen-Orr, R. Milo, S. Mangan, and U. Alon, Nat. Genet. **31**, 64 (2002).
[3] M. Reigl, U. Alon, and D. B. Chklovskii, BMC Evol. Biol. **2**, 25 (2004).
[4] S. Song, P. J. Sjöström, M. Reigl, S. Nelson, and D. B. Chklovskii, PLoS Biol. **3**, e68 (2005).
[5] U. Alon, *An Introduction to System Biology: Design Principles of Biological Circuits* (Chapman and Hall, London, 2006).
[6] S. Wuchty, Z. N. Oltvai, and A.-L. Barabási, Nat. Genet. **35**, 176 (2003).
[7] O. Sporns and R. Kotter, PLoS Biol. **2**, e369 (2004).
[8] U. Alon, Nature (London) **446**, 497 (2007).
[9] P. Dayan and L. F. Abbott, *Theoretical Neuroscience: Computational and Mathematical Modeling of Neural Systems* (MIT Press, Cambridge, MA, 2001).
[10] C. G. Li, L. N. Chen, and K. Aihara, PLoS Biol. **2**, e103 (2006).
[11] C. S. Zhou and J. Kurths, Chaos **13**, 401 (2003).
[12] J. M. Casado, Phys. Lett. A **310**, 400 (2003).
[13] L. C. Yu, Y. Chena, and Pan Zhang, Eur. Phys. J. B **59**, 249 2007.
[14] J. J. Collins, C. C. Chow, and T. T. Imhoff, Nature (London) **376**, 236 (1995).
[15] P. C. Gailey, A. Neiman, J. J. Collins, and F. Moss, Phys. Rev. Lett. **79**, 4701 (1997).
[16] D. T. W. Chik, Y. Q. Wang, and Z. D. Wang, Phys. Rev. E **64**, 021913 2001.
[17] S. G. Lee and S. Kim, Phys. Rev. E **60**, 826 (1999).
[18] A. S. Pikovsky and J. Kurths, Phys. Rev. Lett. **78**, 775 (1997).
[19] B. Lindner and L. Schimansky-Geier, and A. Longtin, Phys. Rev. E **66**, 031916 (2002).
[20] Q. S. Li and Y. Gao, Phys. Rev. E **77**, 036117 (2008).
[21] X. J. Sun, M. Perc, Q. S. Lu, and J. Kurths, Chaos **18**, 023102 (2008).
[22] C. Zhou, J. Kurths, and B. Hu, Phys. Rev. Lett. **87**, 098101 (2001).
[23] L. Gammaitoni, P. Häggi, P. Jung, and F. Marchesoni, Rev. Mod. Phys. **70**, 223 (1998).
[24] K. Wiesenfeld and F. Jaramillo, Chaos **8**, 539 (1998).
[25] K. Wiesenfeld and F. Moss, Nature (London) **373**, 33 (1995).
[26] H. Gang, T. Ditzinger, C. Z. Ning, and H. Haken, Phys. Rev. Lett. **71**, 807 (1993).

[27] J. K. Douglass, L. Wilkens, and F. Moss, Nature (London) **365**, 337 (1993).
[28] E. Manjarrez, J. G. Rojas-Piloni, I. Méndez, L. Martínez, D. Vélez, D. Vázquez, and A. Flores, Neurosci. Lett. Suppl. **326**, 93 (2002).
[29] C. G. Li, Phys. Rev. E **78**, 037101 (2008).
[30] E. M. Izhikevich, IEEE Trans. Neural Netw. **14**, 1569 (2003).
[31] P. E. Kloeden, E. Platen, and H. Schurz, *Numerical Solution of SDE Through Computer Experiments* (Springer-Verlag, Berlin, 1994).
[32] W. Wang, Y. Q. Wang, and Z. D. Wang, Phys. Rev. E **57**, R2527 (1998).
[33] Y. G. Yu, W. Wang, J. Wang, and F. Liu, Phys. Rev. E **63**, 021907 (2001).
[34] Y. G. Yu, F. Liu, and W. Wang, Biol. Cybern. **84**, 227, (2001).